Solid State Ionics 180 (2009) 1061–1068

Contents lists available at ScienceDirect

Solid State Ionics

journal homepage: www.elsevier.com/locate/ssi

Nanoflake CoN as a high capacity anode for Li-ion batteries

B. Das, M.V. Reddy, P. Malar, Thomas Osipowicz, G.V. Subba Rao, B.V.R. Chowdari *

Department of Physics, National University of Singapore, 117 542, Singapore

ARTICLE INFO

Article history:
Received 5 March 2009
Received in revised form 7 May 2009
Accepted 9 May 2009

Keywords:
CoN
Thin films
Electrochemical behavior
Anodes
Li-ion batteries

ABSTRACT

CoN films with nanoflake morphology are prepared by RF magnetron sputtering on Cu and oxidized Si substrates and characterized by X-ray diffraction (XRD), field-emission scanning electron microscopy (FE-SEM), high resolution transmission electron microscopy (HR-TEM) and selected area electron diffraction (SAED) techniques. The thickness and composition of the films are determined by the Rutherford back scattering (RBS) technique confirming the stoichiometric composition of CoN with a thickness, 200 (±10) nm. Li-storage and cycling behavior of nanoflake CoN have been evaluated by galvanostatic discharge–charge cycling and cyclic voltammetry (CV) in cells with Li–metal as counter electrode in the range of 0.005–3.0 V at ambient temperature. Results show that a first-cycle reversible capacity of 760 (±10) $mAhg^{-1}$ at a current rate 250 mAg^{-1}(0.33 C) increases consistently to yield a capacity of 990 (±10) $mAhg^{-1}$ after 80 cycles. The latter value corresponds to 2.7 mol of cyclable Li/mol of CoN vs. the theoretical, 3.0 mol of Li. Very good rate capability is shown when cycled at 0.59 C (up to 80 cycles) and at 6.6 C (up to 50 cycles). The coloumbic efficiency is found to be 96–98% in the range of 10–80 cycles. The average charge and discharge potentials are 0.7 and 0.2 V, respectively for the decomposition/formation of Li_3N as determined by CV. However, cycling to an upper cut-off voltage of 3.0 V is essential for the completion of the "conversion reaction". Based on the ex-situ-XRD, -HR-TEM and -SAED data, the plausible Li-cycling mechanism is discussed. The results show that nanoflake CoN film is a prospective anode material for Li-ion batteries.

1. Introduction

Lithium ion batteries (LIBs) as dominant dc power sources for the mobile communication devices and portable computers, have attracted attention due to their high energy density and rechargeability over a large number of discharge–charge cycles [1–4]. Specialty graphite is used as the anode (negative electrode) with a theoretical capacity of 372 $mAhg^{-1}$ in the commercial first-generation LIBs. Graphite works on the basis of Li-ion intercalation–deintercalation reaction during the charge–discharge operation, the Li-ions coming from the cathode, a mixed oxide, $LiCoO_2$. However, for the application of LIBs to portable power tools and electric vehicles/hybrid electric vehicles (EV/HEV), a higher energy density and safety-in-operation are needed, and hence a lot of research effort has been expended during the last decade to find alternative anode materials which can yield high reversible capacities and which may work on a reaction mechanism which is different from the intercalation–deintercalation process. As a result, metals or their compounds which can form alloys with Li (e.g., $Sn + 4.4\ Li \leftrightarrow Li_{4.4}Sn$), and compounds which can reversibly react with Li via "conversion" reaction (e.g., $CoO + 2\ Li \leftrightarrow Co + Li_2O$), have been found to give reversible capacities which are higher, by a factor two or three, than the theoretical capacity of graphite [1,2,4].

Recent studies have shown that the conversion reactions occur not only with CoO [5], but also with other transition metal oxides like, Fe_2O_3 [6], Fe_3O_4 [7], complex oxides like, MnV_2O_6 [8], $ZnCo_2O_4$ [9], and nano-size particles of these oxides were found to be beneficial in sustaining large number of discharge–charge cycles at various current rates. Also, transition metal compounds with other anions like, fluorides [10–12], oxyfluorides [13], sulphides [14], carbonates [15], phosphides [16,17], and antimonides [14,18] do undergo conversion reactions.

Metal nitrides are attractive materials as prospective anodes since the Li_3N that is formed by the conversion reaction, is an excellent ionic conductor [19], and satisfies one of the essential criteria for a desirable anode. In the literature, ternary metal nitrides of the general formula, $(Li_{3-x}M_x)N$, M = Fe, Co, Ni, Cu [20–24] and LiNiN [25] have been explored for their Li-cyclability. Many binary metal nitrides, in thin film form, have been examined by the group of Fu: Ni_3N [26] and Fe_3N [27] showed reversible capacities ranging from 324 to 420 $mAhg^{-1}$. Studies on thin films of CrN [28] and recently, $(Cr_{1-x}Fe_x)N$, $x = 0$–1 [29] and of VN [30] by the same group showed initial reversible capacities in excess of 1000 $mAhg^{-1}$ when cycled in the voltage range, 0.01–3.5 V vs Li. While CrN retained ~1000 $mAhg^{-1}$ after 30 cycles, with significant electrode-polarization, films of the composition, $x = 0.17$ in $(Cr_{1-x}Fe_x)N$ and VN showed a stable capacity of

* Corresponding author. Tel.: +65 6516 2531; fax: +65 6777 6126.
E-mail address: phychowd@nus.edu.sg (B.V.R. Chowdari).

0167-2738/$ – see front matter © 2009 Elsevier B.V. All rights reserved.
doi:10.1016/j.ssi.2009.05.007

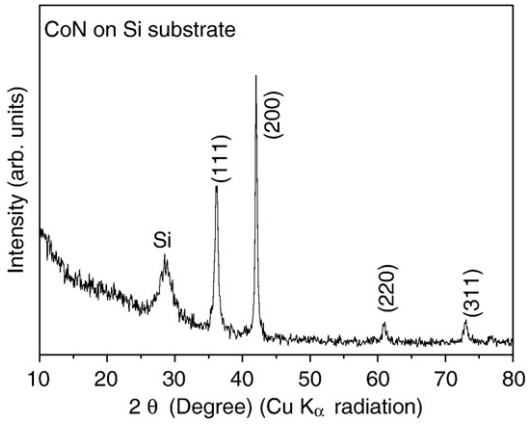

Fig. 1. X-ray diffraction pattern (XRD) of nanoflake CoN grown on surface-oxidized Si substrate. The line due to Si substrate is shown. Miller indices (*h k l*) of CoN are shown.

$\geq$800 mAhg^{-1} in the range 10–50 cycles. The proposed Li-cycling reaction mechanism, substantiated by complementary ex-situ studies, involves the conversion reaction:

$$MN + 3Li^{+} + 3e^{-}(\text{electron}) \leftrightarrow M + Li_3N (M = Cr, V, Fe) \quad (1)$$

It will be of interest to examine other binary metal nitrides for their Li-cyclability. Presently, we prepared thin films of CoN on Cu-substrates, characterized and studied the discharge–charge characteristics at various current (*C*) rates up to 80 cycles. Results show reversible capacities over 950 mAhg^{-1} after 80 cycles at 0.33 *C* and 0.59 *C* rates, whereas a capacity of 650 mAhg^{-1} is shown after 50 cycles at 6.6 *C* rate. Complementary cyclic voltammetry and ex-situ X-ray diffraction and HR-TEM data are also presented.

2. Experimental section

The CoN thin films were deposited on Cu-foil substrates (16 mm in diameter, and 20 μm thick discs, 99.9%) and on surface oxidized Si-substrates (SHE, Japan; 6.25 cm^2 area and 380 μm thick) by using RF magnetron sputtering (Denton Vacuum Discovery 18 system) in N_2 atmosphere. Both the substrates were contained in the sputtering chamber. The Co–metal disc (Angstrom Sciences, 99.9%) was used as the target. The deposition conditions are: RF power at 150 W, N_2 partial pressure at 10 mTorr, sputtering time, 120 min and substrate temperature, 27 °C. Several films of CoN, of thickness ~200 nm were deposited on the above substrates. The CoN films were characterized by X-ray diffraction (XRD) using Philips X'PERT MPD unit (Cu K_α radiation), Field emission scanning electron microscopy (FE-SEM) (JEOL JSM-6700F), High resolution transmission electron microscopy (HR-TEM) and Selected area electron diffraction (SAED) (JEOL JEM 3010 operating at 300 kV).

The Rutherford back scattering measurements were carried out using the accelerator facility at the Centre for Ion Beam Applications laboratory. A 2 MeV He^+ beam with a 2 mm diameter and a current of 10 nA was used for the measurements at room temperature. The energy of the backscattered particles were recorded using the 50 mm^2 passivated implanted planar silicon (PIPS) detectors with an energy resolution of ~18 keV. The detector was positioned at 170° scattering angle. The experimental data were analyzed using the simulation software XRUMP [31] to determine the composition and thickness of the films.

For electrochemical measurements, the virgin CoN films grown on Cu-substrate were used as the electrodes. The active mass of the electrode was calculated by using the theoretical density of CoN (6.106 g cm^{-3}) and the geometrical area of the electrode, 2 cm^2 and was found to be, typically, ~0.24 mg. The electrodes were dried in a vacuum oven overnight at ~70 °C and transferred to Ar-filled glove box (MBraun, Germany) for the cell assembly. The atmosphere in the glove-box was maintained at <1 ppm of H_2O and O_2. Coin cells (size 2016; 20 mm in diameter and 1.6 mm thick) were assembled using the CoN as the cathode, a glass microfiber filter (GF/F) (Whatman Int. Ltd, Maidstone, England) as the separator and the electrolyte, 1M $LiPF_6$ dissolved in ethylene carbonate (EC) + diethyl carbonate (DEC) in the ratio of 1:1 volume (Merck). The Li–metal foil (Kyokuto Metal Co., Japan) was cut in to circular discs (16 mm diameter) and used as the counter electrode. More details on the cell fabrication are described elsewhere [32]. The fabricated cells were aged for 12 h before measurement to ensure penetration of electrolyte into the active material. The galvanostic cycling and cyclic voltammetry were carried out at room temperature using multichannel battery tester (model SCN, Bitrode, USA) and Macpile II system (Biologic, France), respectively. For the ex-situ XRD patterns of the discharged and cycled electrodes, the cells were disassembled in the glove box, the electrodes were recovered, washed with DEC, dried, covered with paraffin film to protect them from exposure to air/moisture and mounted on the XRD instrument. For ex-situ TEM studies, the electrode material was scraped from the Cu-foil in the glove box and the powder was dispersed in ethanol by ultrasonic miller (Transsonic, 660/H, Germany) and deposited on to a holey carbon coated Cu grid. More details on sample preparation for ex- situ XRD and TEM are reported elsewhere [15,32].

3. Results and discussion

3.1. Structural and morphological characterization

Suzuki et al [33] have prepared thin films of CoN by dc reactive sputtering and studied their crystal structure and magnetic properties. They found that CoN adopts a cubic zinc blende-type structure with $a = 4.297$ Å. Fig. 1 shows the XRD pattern of CoN thin film deposited on surface oxidized Si (111) substrate. The Miller indices (*h k l*) correspond to the cubic structure with the space group, $F\,\bar{4}3\,m$. The lattice parameter was calculated by using least square fitting of 2θ and (*h k l*) values and found to be $a = 4.291\ (5)$ Å, in good agreement with the reported value of 4.297 Å [33] [JCPDS card no. 83-0831]. The XRD pattern of the CoN film deposited on the Cu-substrate is shown in Fig. 2. Because of the preponderance of the intensities of the lines due to the Cu-substrate and the Al-sample holder, the characteristic lines due to CoN are of low relative-intensity. However, the lines due to

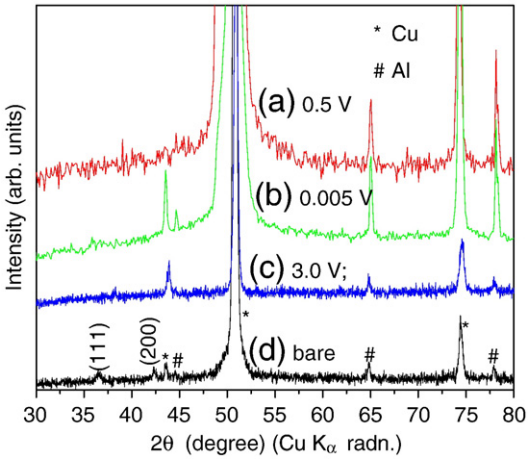

Fig. 2. XRD patterns of the bare CoN electrode grown on Cu-substrate and those of the electrodes of CoN discharged to 0.5 and 0.005 V, and charged to 3.0 V at the end of 1st cycle. Miller indices assigned to the peaks of bare CoN are shown. The symbols (*,#) represent the lines due to Cu–metal (electrode substrate) and Al–metal (sample holder). The *y*-axis values are normalized for better comparison of the XRD patterns.

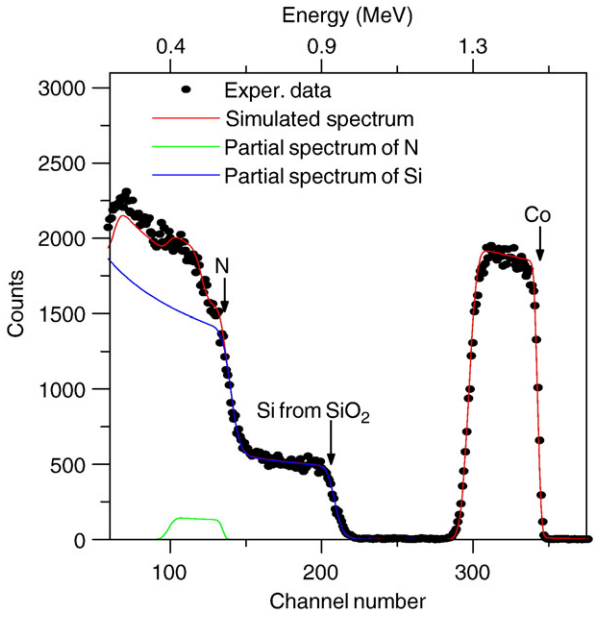

Fig. 3. Rutherford back scattering (RBS) spectrum of nanoflake CoN grown on surface-oxidized Si substrate. The simulated partial spectra due to the individual elements are indicated.

Miller indices (111) and (200) can be clearly seen, which are in agreement with those shown in Fig. 1.

Rutherford back scattering (RBS) or more accurately, elastic back scattering is a valuable technique that can give information on the chemical composition, and in the case of thin films, their thickness [34]. Briefly, in a typical experiment the sample (e.g., thin film deposited on a substrate) is exposed to a beam of fast ions, like He^+ ions. The ions will collide with both the surface atoms as well as those present in the bulk, up to a certain depth, and get back-scattered. The mass ratio of the ions and the colliding target atom together with scattering angle (170°) will determine the kinetic energies of the back-scattered ions. The RBS spectrum displays the number of back-scattered ions vs. energy or channel number. Because the scattering probability is quantitatively known, with an appropriate simulation code (XRUMP), one can extract composition and thickness of thin film systems. Fig. 3 shows a typical 2 MeV RBS spectrum obtained for the CoN film on surface oxidized Si-substrate. In the figure, the full circles are the experimental data and the continuous lines denote the simulated data using the XRUMP [31]. The back scattering surface energies of different elements present in the sample are indicated in the spectrum. Apart from the total simulated spectrum, the partial spectra of silicon and nitrogen are also shown indicating the components of the overlapped region. The atomic percentage values obtained for cobalt (50 at.%) and nitrogen (50 at.%) from the simulations confirm the stoichiometry of the CoN films. The thickness

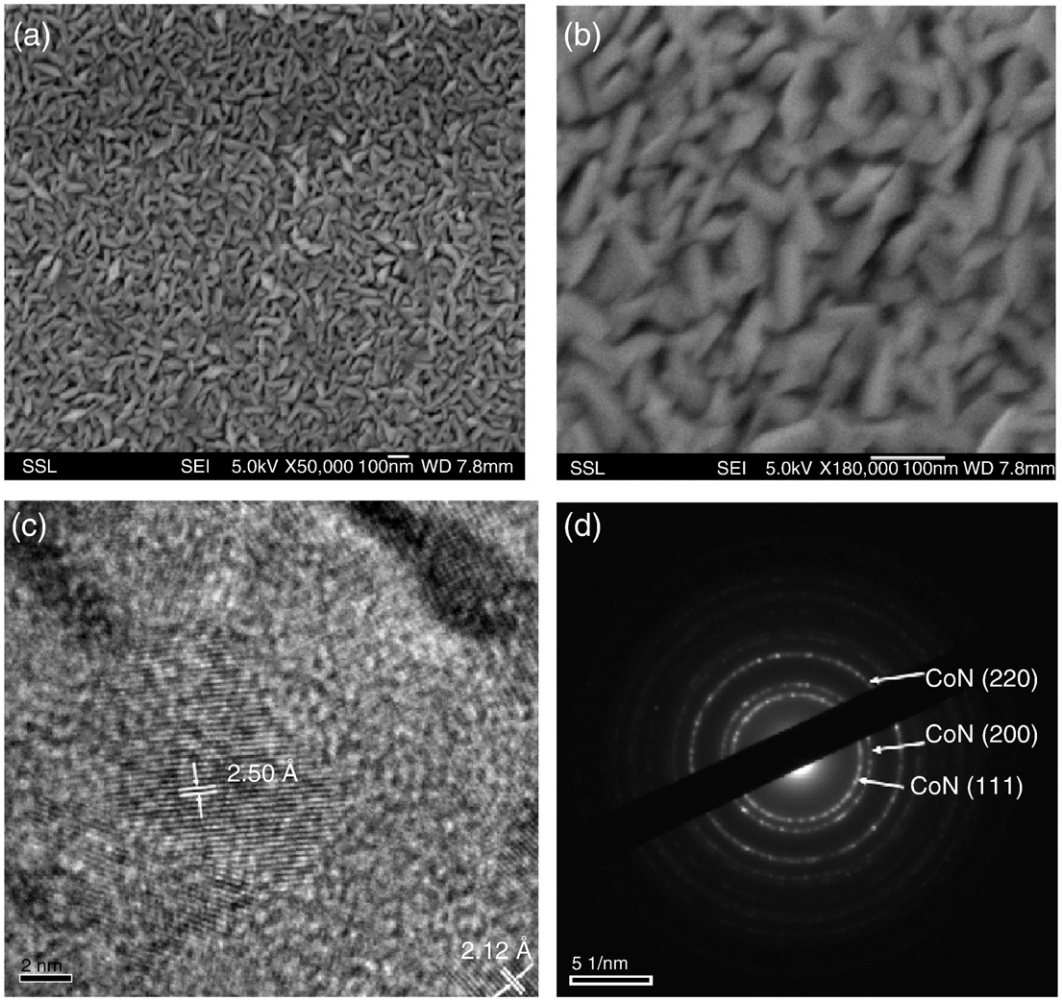

Fig. 4. (a, b) FE-SEM photographs of nanoflake CoN grown on Cu-substrate at two different magnifications showing randomly oriented nanoflakes of size ≤100 nm. (c) HR-TEM lattice image of nanoflake CoN. The interplanar (*d*-) spacings are indicated by arrows. (d) The SAED pattern of nanoflake CoN. Miller indices are indicated. Scale bars are shown.

of the film was found to be 200 (±10) nm. The bulk density of 6.106 g cm^{-3} of CoN was used in calculating the thickness. We assume that the chemical composition and thickness of the CoN films deposited on Cu-substrate are identical to those deposited on oxidized Si-substrates, since both the films were deposited under the same conditions in the sputtering chamber.

The FE-SEM photographs of the CoN nanoflakes grown on Cu-foil are shown in Fig. 4 a, b. As can be seen, nanoflakes of size ≤100 nm are densely packed but are randomly oriented with an aspect ratio, 10:1. The HR-TEM lattice image and SAED pattern of the CoN film are shown in Fig. 4 c,d. Randomly oriented crystalline-regions and some amorphous regions are clearly seen. The *d*-spacings (inter planar distances) of the planes in Fig. 4c are 2.50 (±0.02) and 2.12 (±0.02) Å and these correspond to the Miller indices (111) and (200), respectively of CoN (Fig. 1). The SAED pattern shows highly resolved concentric diffuse rings and some bright spots (Fig. 4d). The diffuse rings indicate the nano-phase nature of CoN. The calculated *d*-values from the rings are: 2.50, 2.12 and 1.49 (±0.02) Å and these correspond to the (*h k l*) values (111), (200) and (220), respectively. Thus, from the above data, we conclude that the CoN films consist of nanoflakes of size ≤100 nm, densely packed with a total layer thickness, 200 (±10) nm.

3.2. Electrochemical properties

3.2.1. Galvanostatic cycling

The discharge–charge profiles (voltage vs. capacity curves) of nanoflake CoN at a current density 250 mAg^{-1} (0.33 C) in the voltage window, 0.005–3.0 V vs. Li, up to 80 cycles are shown in Fig. 5a, b. During the first discharge, that is, reaction with Li, the voltage drops from the open circuit voltage (OCV~2.6 V) continuously with small and broad plateaus at ~1.3 and at ~0.8 V. At this point, the capacity is ~300 $mAhg^{-1}$ which corresponds to the consumption of ~0.8 mol of Li/mol of CoN. After this, a large voltage plateu is observed at ~0.6 V up to a capacity of 570 $mAhg^{-1}$ (1.6 mol of Li) followed by a gradual decrease in voltage up to the deep discharge limit, 0.005 V. The total first discharge capacity is 1080 (±10) $mAhg^{-1}$ (2.94 mol of Li). This value is close to the theoretical capacity of 1102 $mAhg^{-1}$ (3 mol of Li as per Eq. (1)) expected from the complete reaction of CoN with Li and formation of Co–metal nano particles and Li_3N [26–30]. The first charge profile (extraction of Li) comprises a fairly large voltage plateu at ~0.7 V, with capacity ~350 $mAhg^{-1}$ (~0.95 mol of Li) followed by a smaller plateu at ~1.3 V. The overall first charge capacity is 760 (±10) $mAhg^{-1}$ (2.07 mol of Li) and thus, the irreversible capacity loss (ICL) observed during the first cycle is 320 $mAhg^{-1}$ (0.87 mol of Li).

The second discharge profile shows a variation from the first-discharge profile indicating a slightly different electrode reaction. The plateau at ~0.6 V noticed during the first discharge is not observed and the plateu at ~0.8 V becomes more prominent (Fig. 5a). The total second discharge capacity observed is 780 (±10) $mAhg^{-1}$ (2.12 mol of Li). The second charge profile is analogous to the first-charge profile showing a similar cycling behavior and the charge capacity is 755 (±10) $mAhg^{-1}$, almost the same as the first- charge capacity. With an increase in the cycle number, the reversible capacity decreases slightly. However, after 5 cycles, it increases slowly but consistently

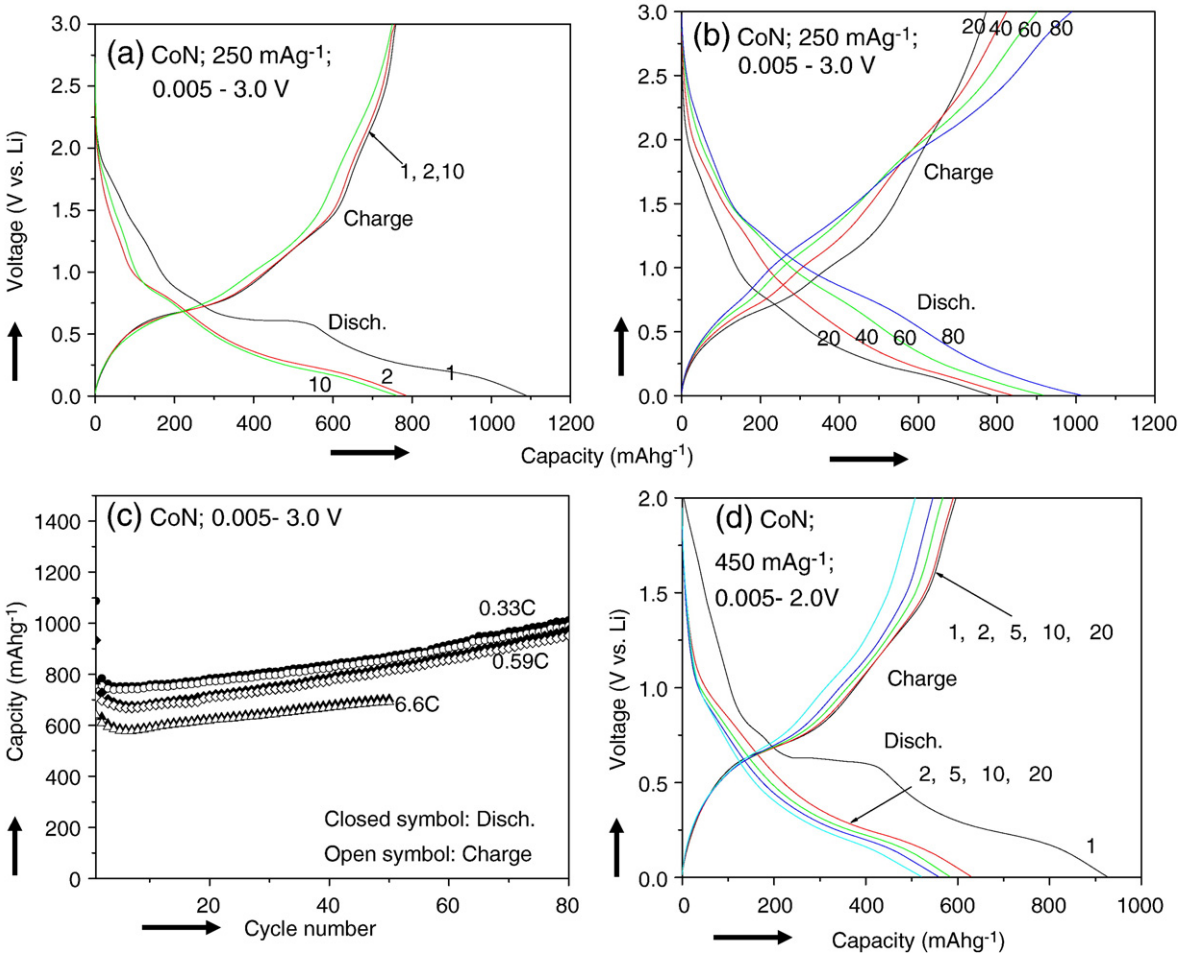

Fig. 5. Galvanostatic discharge–charge curves of nanoflake CoN: (a) 1–10 cycles and (b) 20–80 cycles, at 250 mAg^{-1} (0.33 C) in the range of 0.005–3.0 V. Only selected cycles are shown for clarity. Numbers indicate cycle number. (c) Capacity vs. cycle number (up to 80 cycles) plots of nanoflake CoN. Voltage range, 0.005–3.0 V vs. Li, at *C*-rates of 0.33, 0.59 and 6.6 *C*. (d) Discharge–charge profiles of nanoflake CoN up to 20 cycles at 450 mAg^{-1} (0.59 C) in the range of 0.005–2.0 V. The numbers indicate cycle number.

to 990 (±10) $mAhg^{-1}$ at the end of 80th cycle (Fig. 5b, c). Assuming 1 C = 760 mAg^{-1}, the current rate of 250 mAg^{-1} corresponds to 0.33 C [35]. There is also a qualitative change in the discharge–charge profiles in the cycling range, 20–80 cycles: The well-defined voltage plateau regions are absent and show somewhat smoothly varying curves (Fig. 5b). In order to establish the rate capability of the nanoflake CoN films, galvanostatic cycling was carried out on duplicate cells at 450 mAg^{-1} (0.59 C) up to 80 cycles, and at 5000 mAg^{-1} (6.6 C) up to 50 cycles at room temperature. The voltage-capacity profiles are similar to those shown in Fig. 5a, b. The capacity vs cycle number plots are shown in Fig. 5c. As can be expected, the reversible capacities are smaller in comparison to those measured at 0.33 C. However, the general trend of the cycling behavior is similar. That is, there is an initial decrease in the capacity up to a few cycles, followed by a consistent increase up to the end of cycling. Thus, at 0.59 *C*-rate, the capacity increases from 670 $mAhg^{-1}$ at the 5th cycle to 950 (±10) $mAhg^{-1}$ (2.6 mol of Li) at the 80th cycle. Similarly, at 6.6 *C*-rate, the reversible capacity increases from 570 $mAhg^{-1}$ at the 5th cycle to 690 (±10) $mAhg^{-1}$ (1.9 mol of Li) at the 50th cycle. From Fig. 5c, it can be seen that the discharge and charge capacities overlap well and the coulombic efficiency (η) is 96–98%.

Galvanostatic cycling was also carried out on duplicate cells at 450 mAg^{-1} (0.59 C) up to 20 cycles, in the voltage window 0.005–2.0 V vs Li, in order to see the effect of reducing the upper cut-off voltage. The voltage-capacity profiles, shown in Fig. 5d, are qualitatively similar to those in Fig. 5a, b. The total first-discharge capacity is 925 (±10) $mAhg^{-1}$ (~2.5 mol of Li), whereas the first-charge capacity is 595 (±10) $mAhg^{-1}$. The ICL is thus 330 $mAhg^{-1}$ and compares well with the value of 320 $mAhg^{-1}$ obtained at 0.33C, with the upper voltage cut-off of 3.0 V (Fig. 5a). However, the capacity decreased consistently in the range 2–20 cycles, reaching a value of 505 (±10) $mAhg^{-1}$ (1.4 mol of Li) at the 20th cycle. Hence, we conclude that cycling to an upper cut-off voltage of 3.0 V is necessary in order to realize the high capacities over extended number of cycles.

It is well-known that the ICL during the first-cycle arises due to the extra consumption of Li, in addition to that needed for the reduction of metal oxide, fluoride, nitride etc to the respective metal nanoparticles (e.g., Eq. (1)), for the formation of solid electrolyte interphase (SEI), and a polymeric layer, under deep discharge conditions, 0.005 V vs Li [5,9,14,36]. The solvents present in the electrolyte, namely EC and DEC participate in the reaction with Li to form the above SEI and polymeric layer. During subsequent discharge and charge cycling, at least up to a certain number of cycles, the latter two re-form and decompose respectively, till a stable structuring of the electrode is attained. This is called "formatting" of the electrode, after which the SEI gets stabilized and the reversibility of the electrode as well as the η are improved. Studies on oxides like CoO [5,14,36] and $ZnCo_2O_4$ [9] have shown that in order to realize the maximum obtainable reversible capacities during cycling, it is essential to employ an upper cut-off voltage of ≥3.0 V vs Li. This is to enable the decomposition of the polymeric layer formed (or re-formed under deep discharge) on the nano-particles of the active material. As can be seen from Fig. 5b, c and d, cycling up to 3.0 V is essential to obtain high and reversible capacities in CoN. We note that the group of Fu

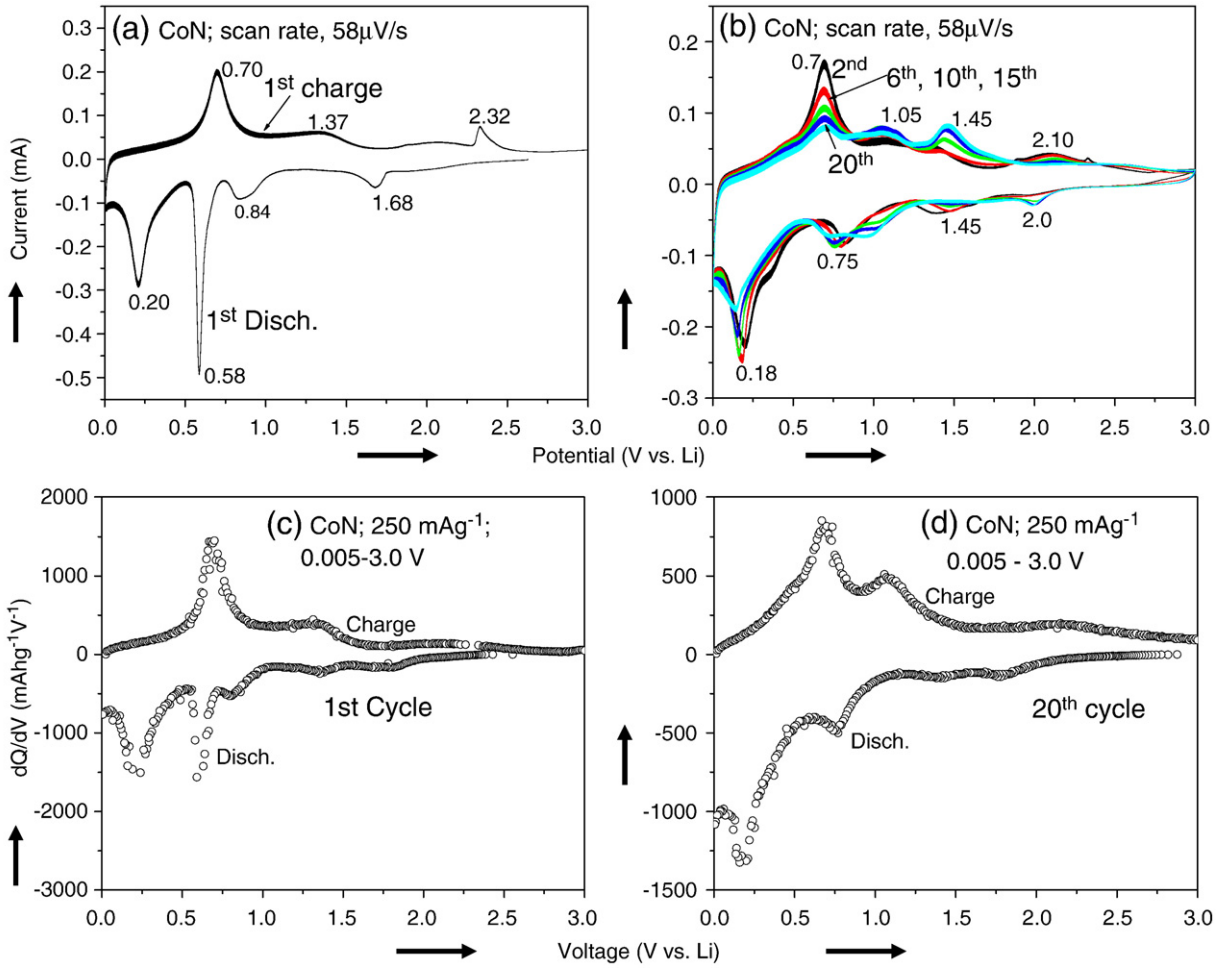

Fig. 6. Cyclic voltammograms of nanoflake CoN: (a) 1st cycle and (b) 2–20 cycles. Only selected cycles are shown for clarity. Scan rate is 58 μVs^{-1}. Li–metal anode is the counter and reference electrode. Numbers represent the potentials in Volts. (c) Differential capacity (dQ/dV) vs. Voltage plot for the first-cycle extracted from the galvanostatic capacity-voltage profiles of Fig. 5a. (d) Differential capacity (dQ/dV) vs. Voltage plot for the 20th-cycle extracted from the galvanostatic capacity- voltage profiles of Fig. 5b.

employed an upper cut-off voltage of 3.5 V vs Li for CrN [28], $(Cr_{1-x}Fe_x)N$ [29] and VN [30] and obtained high reversible capacities.

3.2.2. Cyclic voltammetry

Cyclic voltammetry studies act as complementary tool to the galvanostatic cycling data in establishing the voltages at which the reactions occur and the existence of two-phase region. The cyclic voltammograms (CV) were recorded in the potential range 0.005–3.0 V, at the slow scan rate of 58 μV/s up to 20 cycles and are shown in Fig. 6a, b. The Li metal is used as the counter and reference electrode. As can be seen in Fig. 6a, during the first cathodic scan (reaction of Li with CoN), starting from OCV (~2.6 V) a smooth sloping curve up to ~1.7 V is observed with low intensity peaks at 1.68 V and 0.84 V. This is an indication of single phase reaction and reduction of Co^{3+} in CoN forming Li_x(CoN). The low-intensity peaks may represent phases with different values of x or phase transitions in Li_x(CoN). An intense cathodic (reduction) peak is observed at 0.58 V, followed by another strong peak at 0.2 V. As will be discussed later, these peaks represent the structure- destruction followed by the formation of Co–metal and Li_3N in a two-phase reaction. During the first anodic scan (Li extraction), the CV shows a strong peak at 0.7 V followed by minor peaks at 1.37 and 2.32 V (Fig. 6a). These peaks are the indication of decomposition of Li_3N and formation of CoN (reverse reaction of Eq. (1)).

The second cathodic scan differs from the first one in that the peak at 0.58 V is absent and all the other cathodic peaks show minor shifts in potentials (Fig. 6b). In the second anodic scan, the intense peak at 0.7 V appears as in the first anodic scan and the minor anodic peaks now appear at 1.05 V and 2.10 V. With an increase in the cycle number, the CVs overlap well showing good reversibility. However, development of minor additional peaks at 1.45 V and 1.0 V in the cathodic scans, and a peak at ~1.45 V in the anodic scans are clearly noted. The low-intensity multiple peaks in the cathodic/ anodic scans are an indication of intermediate step-reactions for the decomposition/ formation of CoN during cycling. The differential capacity (dQ/dV) vs. voltage plots for the first and 20th cycle are shown in Fig. 6c and d. These are extracted from the galvanostatic capacity vs. voltage profiles of Fig. 5a and b, respectively. The voltage plateau regions in the latter profiles appear as peaks in Fig. 6c and d, respectively. As is clear, they show an excellent resemblance to the CVs in Fig. 6a and b, both in the shape as well as the values of the peak potentials, thereby confirming the complementary nature of the CVs, and reproducibility of the electrochemical properties of the CoN–Li system. From the data of Fig. 6, we note that the formation and decomposition of Li_3N occurs at potentials ~0.2 and ~0.7 V, respectively. The decomposition and formation of CoN occurs mainly at potentials ~0.75 and ~1.05 V, respectively (Fig. 6a,b). However, the existence of several low-intensity peaks in the range, 1.0–2.1 V, both in the cathodic and anodic scans indicate that the "conversion" reaction involves the formation of intermediate compositions, $(Li_{3-x}Co_x)N$ (e.g., $x=0.1$–0.44 [20,21]), and cycling up to 3.0 V is essential for the realization of full reversible capacity. We may mention here that Gillot et al [37] and Boynov et al [38] have shown that in the NiP_2–Li system, Li-cyclability occurs through the formation/ decomposition of an intermediate phase, Li_2NiP_2.

3.2.3. Ex-situ XRD, TEM and SAED

Studies by the group of Fu on CrN [28], $(Cr_{1-x}Fe_x)N$ [29] and VN [30] have shown that the crystal structure destruction occurs during the first discharge due to the reaction of Li with the starting materials followed by the formation of nano-size metals and Li_3N. Subsequent charging will re-form VN releasing Li-ions and electrons (reverse reaction of Eq. (1)). In order to confirm the crystal structure destruction in the case of CoN, several identical cells were assembled and then discharged /charged to selected voltages. After stabilizing for about 2 h, the cells were disassembled in the glove box and treated as described in experimental section. The XRD patterns of the electrodes during the first cycle are shown in Fig. 2. The relative intensities (*y*-axis) have been normalized for better comparison. The XRD pattern of electrode discharged to 0.5 V did not show any peaks of CoN and peaks due to Cu-substrate and Al-sample holder only are seen. This shows the structure destruction started slightly above 0.5 V and corroborates the galvanostatic and CV data where a large voltage plateau sets in at ~0.58 V indicating two-phase reaction. The XRD pattern at 0.005 V during the first-discharge is also devoid of any peaks indicating that the electrochemically-formed species (Co–metal and Li_3N) are not noticeable, due to their nano size nature [9,15,28,30]. Similarly, the XRD pattern taken at 3.0 V at the end of first-charge also does not show any characteristic peaks due to CoN.

The ex-situ HR-TEM lattice image and the SAED pattern of the CoN electrode in the fully charged state (3.0 V) after 80 cycles are shown in Fig. 7a and b, respectively. Fig. 7a compares well with the lattice image of virgin CoN film of Fig. 4c and shows the nano-crystalline grains (~3–5 nm) embedded in an amorphous matrix. The interplanar *d*-spacing is found to be 2.51(±0.02) Å, which corresponds to the (111) plane of CoN. The grain-size reduction of the embedded particles in an amorphous matrix is due to the so called "electrochemical grinding" effect [14]. The SAED pattern comprises a diffuse set of concentric rings with some bright spots indicating low-crystallinity of CoN (Fig. 7b). The *d*-values calculated from the rings are 2.51, 2.13 and 1.45 (±0.02) Å and correspond to the (*h k l*) values (111), (200) and (220), respectively of CoN. These values are in good

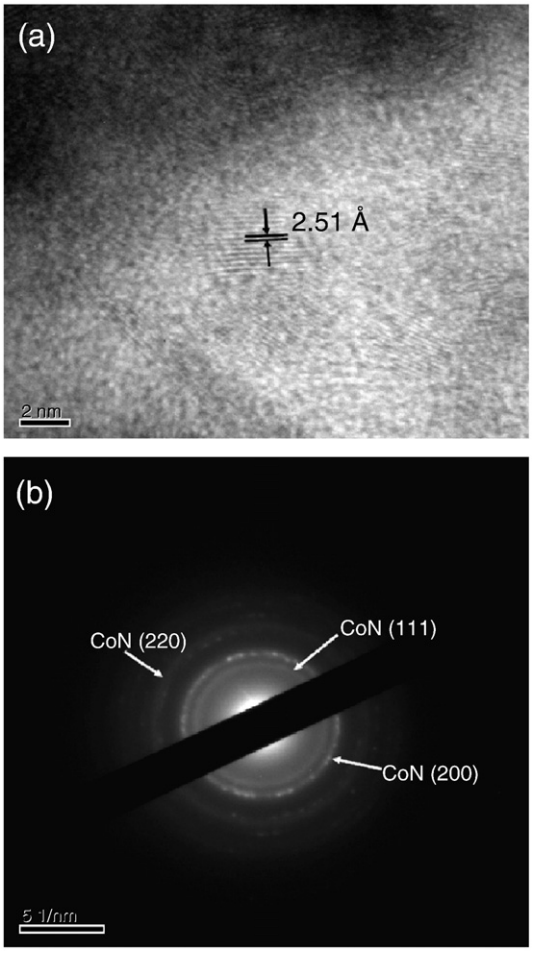

Fig. 7. (a) HR-TEM lattice image and (b) SAED pattern of cycled electrode nanoflake CoN in the charged state (3.0 V) after 80 cycles in the range, 0.005–3.0 V vs. Li. The *d*-spacing is shown by arrows. The Miller indices of CoN are indicated. Scale bars are shown.

agreement with the *d*-values calculated from the XRD pattern and the SAED of virgin material shown in Fig. 4d. Thus, from the ex-situ XRD, -HR-TEM and -SAED data, we conclude that during the discharge process, CoN decomposes to Co and Li_3N whereas during the charging process, re-formation of CoN occurs. We note, however, that some unreacted CoN may also be contributing to the observed data, and hence, ex-situ HR-TEM and -SAED on the discharged-product after 80 cycles, is also necessary to substantiate the above statement.

3.3. Reaction mechanism

Based on ex-situ XRD, HR-TEM and SAED patterns and the observed galvanostatic cycling and CV data, a Li- cycling mechanism can be proposed similar to that established by Sun and Fu for the metal nitrides, CrN [28] and VN [30] except for an intermediate step during the first-discharge involving Li-intercalation, Eq. (2):

$$CoN + 0.8Li^+ + 0.8e^- \rightarrow Li_{0.8}CoN \quad (2)$$

$$Li_{0.8}CoN + 2.2Li^+ + 2.2e^- \rightarrow Co + Li_3N \quad (3)$$

$$Co + Li_3N \leftrightarrow CoN + 3Li^+ + 3e^- \quad (4)$$

The reaction in Eq. (2) is supported by the galvanostatic cycling (Fig. 5a) and CV (Fig. 6a), where a smoothly varying voltage profile is noted up to ~0.6 V during the first- discharge, with minor voltage plateaus observed at ~1.3 V and ~0.8 V, and consumption of 0.8 mol of Li (capacity of ~300 $mAhg^{-1}$). The broad voltage plateau appearing both in the galvanostatic profile (Fig. 5a), and as a peak in CV (Fig. 6a) at 0.58 V indicates the crystal structure destruction (amorphisation) followed by Eq. (3), indicating the co-existence of intercalated phase ($Li_{0.8}CoN$), Co and Li_3N. This is well-supported by the ex-situ XRD (Fig. 2). The XRD peaks due to Co and Li_3N are not seen due to their nano size nature.

The theoretical reversible capacity based on the reaction mechanism Eq. (4) is 1102 $mAhg^{-1}$ (3 mol of Li), but the experimental first-discharge capacity observed is 1080 (±10) $mAhg^{-1}$ (2.94 mol of Li). As discussed earlier, considerable amount of Li will also be consumed during the first-discharge for the formation of SEI and polymeric layer on the freshly generated Co–metal nano-particles. Hence, we assume an incomplete participation of the active material during the first-discharge. The first-charge process can be represented by the forward reaction of Eq. (4), analogous to Eq. (1). The first-charge capacity is only 760 $mAhg^{-1}$ (2.06 mol of Li) which indicates that ~0.9 mol of Li might have been consumed for the formation of SEI and polymeric layer. The second and subsequent cycling involve only Eq. (4) and do not appear to go through Eq. (2), due to the continuous decrease in the width of the voltage plateau at ~0.6 V (Fig. 5a,b and d). With an increase in the cycle number, both the discharge and charge capacities show a systematic increase, indicating an increase in the participation of the "active material" in each cycle, ultimately reaching 990 $mAhg^{-1}$ (2.7 mol of Li) at 0.33 *C* rate, at the end of 80th cycle. We note, however, that neither the theoretical reversible capacity nor the observed first-discharge capacity have been achieved till the 80th cycle, indicating that full participation of the "active material" possibly needs cycling beyond 80 cycles. The same trend is shown when cycled at both 0.59 *C* and 6.6 *C* rates (Fig. 5c). An increase in the reversible capacity with an increase in the cycle number has been observed in several oxide systems in the literature, like $LiMVO_4$, M = metal [39], nano-Fe_3O_4 [7], $LiHoMo_3O_8$ [32] and $LiYMo_3O_8$ [40]. An explanation similar to that for CoN can be given for the observed cycling behavior of the above compounds.

It is relevant to compare the present data on nanoflake CoN with those reported by Fu and co-workers on thin films of CrN [28], FeN [29] and VN [30]. Their thin films varied in thickness from 400 to 700 nm, and TEM showed smooth films without any characteristic morphology. They found that, when cycled at 28 $\mu A/cm^2$ (~230 mAg^{-1}, based on the weight of the film) in the range 0.005–3.5 V vs Li, CrN showed a first cycle charge capacity of 1200 $mAhg^{-1}$ (2.96 mol of Li vs. theoretical 3 mol of Li/formula unit) which slowly degraded at 0.5%/cycle up to 30 cycles. Under similar conditions, films of VN gave a first cycle charge-capacity of 1156 mAh/g, which degraded slowly, but stabilized to 800 $mAhg^{-1}$ (1.94 mol of Li/formula unit) in the range, 15–50 cycles. On the other hand, FeN films showed a first-cycle charge-capacity of 1020 $mAhg^{-1}$, which degraded drastically to 40 $mAhg^{-1}$ after 30 cycles. Thus, we conclude that the cycling performance of nanoflake CoN is comparable to those of thin films CrN and VN, and in addition, shows very good rate-capability.

4. Conclusions

Nanoflake CoN is prepared by RF magnetron sputtering technique and characterized by XRD, RBS, FE- SEM, HR-TEM and SAED techniques. The thickness and composition, analyzed by RBS, confirm the formation of CoN with a thickness, 200 (±10) nm. The Li-cycling behavior of nanoflake CoN is evaluated by galvanostatic discharge–charge cycling and cyclic voltammetry (CV) with Li as the counter electrode at room temperature. When cycled at a current density 250 mAg^{-1} (0.33 C) in the voltage window 0.005–3.0 V, nanoflake CoN film showed an initial reversible capacity of 760 (±10) $mAhg^{-1}$ which increases consistently to 990 $mAhg^{-1}$ (2.7 mol of Li/mol of CoN) at the end of 80th cycle. Excellent rate capability is also shown: At 0.59 C, a capacity of 950 (±10) $mAhg^{-1}$ (2.6 mol of Li) after 80 cycles, and at 6.6 C, a capacity of 690 (±10) $mAhg^{-1}$ (1.9 mol of Li) at the end of 50 cycles, are observed. The coloumbic efficiency is found to be 96–98% in the range of 10–80 cycles. The average charge potential for the decomposition of Li_3N is 0.7 V whereas the average discharge potential for the formation of Li_3N is 0.2 V vs. Li. However, complete reversibility of Eq. (4) requires cycling to an upper cut-off voltage of 3.0 V and appears to go through intermediate phases, $(Li_{3-x}Co_x)N$. The observed galvanostatic cycling, CV and ex-situ-XRD, -TEM and -SAED data have been interpreted in terms of the conversion reaction involving the nano-phase composite "Co–Li_3N". The Li-cycling performance of nanoflake CoN films is compared with those of CrN, FeN, and VN reported in the literature. Thus, the present study shows that nanoflake CoN films can be a prospective anode material for the future generation LIBs.

Acknowledgements

Thanks are due to Mr. G. S. Chen, Department of Physics for the help in making films. Part of the work is supported by Defence Advanced Research Projects Agency (DARPA), USA (Grant no. R-144-000-226-597).

References

[1] G.-A. Nazri, G. Pistoia (Eds.), Lithium Batteries: Science and Technology, Kluwer Academic Publ., New York, 2003.
[2] A.S. Arico, P. Bruce, B. Scrosati, J.-M. Tarascon, W.V. Schalkwijk, Nature Mater. 4 (2005) 366.
[3] P.G. Bruce, B. Scrosati, J.-M. Tarascon, Angew. Chem., Int. Ed. Engl. 47 (2008) 2930.
[4] A.K. Shukla, T. Prem Kumar, Curr. Sci. (India) 94 (2008) 314.
[5] P. Poizot, S. Laruelle, S. Grugeon, L. Dupont, J.-M. Tarascon, Nature 407 (2000) 496.
[6] M.V. Reddy, T. Yu, C.H. Sow, Z.X. Shen, C.T. Lim, G.V. Subba Rao, B.V.R. Chowdari, Adv. Funct. Mater. 17 (2007) 2792.
[7] P.L. Taberna, S. Mitra, P. Poizot, P. Simon, J.-M. Tarascon, Nature Mater. 5 (2006) 567.
[8] D. Hara, J. Shirakawa, H. Ikuta, Y. Uchimoto, M. Wakihara, T. Miyanaga, I. Watanabe, J. Mater. Chem. 12 (2002) 3717.
[9] Y. Sharma, N. Sharma, G.V. Subba Rao, B.V.R. Chowdari, Adv. Funct. Mater. 17 (2007) 2855.
[10] H. Li, P. Balaya, J. Maier, J. Electrochem. Soc. 151 (2004) A1878.

[11] G.G. Amatucci, N. Pereira, J. Fluorine Chem. 128 (2007) 243.
[12] R.E. Doe, K.A. Persson, Y.S. Meng, G. Ceder, Chem. Mater. 20 (2008) 5274.
[13] M.V. Reddy, S. Madhavi, G.V. Subba Rao, B.V.R. Chowdari, J. Power Sources 162 (2006) 1312.
[14] S. Grugeon, S. Laruelle, L. Dupont, J.-M. Tarascon, Solid State Sci. 5 (2003) 895.
[15] Y. Sharma, N. Sharma, G.V. Subba Rao, B.V.R. Chowdari, J. Mater. Chem. (in press). doi:10.1039/b906471k.
[16] D.C.C. Silva, O. Crosnier, G. Ouvrard, J. Greedan, A. S.-Sefat, L.F. Nazar, Electrochem. Solid-State Lett. 6 (2003) A162.
[17] F. Gillot, M. Menetrier, E. Bekaert, L. Dupont, M. Morcrette, L. Monconduit, J.-M. Tarascon, J. Power Sources 172 (2007) 877.
[18] L.M.L. Fransson, J.T. Vaughey, K. Edstrom, M.M. Thackeray, J. Electrochem. Soc. 150 (2003) A86.
[19] T. Lapp, S. Skaarup, A. Hooper, Solid State Ionics 11 (1983) 97.
[20] J.B. Ducros, S. Bach, J.P. P.-Ramos, P. Willmann, Electrochem. Commun. 9 (2007) 496.
[21] J.B. Ducros, S. Bach, J.P. P.-Ramos, P. Willmann, J. Power Sources 175 (2008) 517.
[22] J.B. Ducros, S. Bach, J.P. P.-Ramos, P. Willmann, Electrochim. Acta 52 (2007) 7035.
[23] Y. Liu, T. Mastumura, Y. Ono, N. Imanishi, A. Hirano, Y. Takeda, Solid State Ionics 179 (2008) 2069.
[24] S. Bach, J.P. P.-Ramos, J.B. Ducros, P. Willmann, Solid State Ionics 180 (2009) 231.
[25] J. Cabana, Z. Stoeva, J.J. Titman, D.H. Gregory, M.R. Palacin, Chem. Mater. 20 (2008) 1676.
[26] Y. Wang, Z.-W. Fu, X.-L. Yue, Q.-Z. Qin, J. Electrochem. Soc. 151 (2004) E162.
[27] Z.-W. Fu, Y. Wang, X.-L. Yue, S.-L. Zhao, Q.-Z. Quin, J. Phys. Chem., B 108 (2004) 2236.
[28] Q. Sun, Z.-W. Fu, Electrochem. Solid-State Lett. 10 (2007) A189.
[29] Q. Sun, Z.-W. Fu, Electrochem. Solid-State Lett. 11 (2008) A233.
[30] Q. Sun, Z.-W. Fu, Electrochim. Acta 54 (2008) 403.
[31] L.R. Doolittle, Nucl. Instrum. Methods Phys. Res., B Beam Interact. Mater. Atoms 9 (1985) 344.
[32] B. Das, M.V. Reddy, G.V. Subba Rao, B.V.R. Chowdari, J. Solid State Electrochem. 12 (2008) 953.
[33] K. Suzuki, T. Kaneko, H. Yoshida, H. Morita, H. Fujimori, J. Alloys Compd. 224 (1995) 232.
[34] G. De Roos, J.M. Fluit, L.A.M. Hermans, J.W. Geus, Z. Anorg. Allg. Chem. 449 (1979) 115.
[35] Many reports in the literature defined the 1C-rate as the full discharge or charge capacity corresponding to insertion/extraction of 1mole of Li in 1h. While this is valid for the case of LIB-cathode materials like, $LiCoO_2$, $LiMn_2O_4$ and $LiFePO_4$, we feel that in the case of prospective anode materials which can deliver more than 1Li in 1 h, like CoO, Fe_3O_4, SnO_2, MN (M = V, Cr, Fe and Co), the first-cycle reversible capacity, or in favorable cases, where the reversible capacity which is stable over a large number of cycles, must be used to calculate the C-rate. Thus, we use 1C = 760 mA/g in the case of CoN, since the observed first-cycle reversible capacity is 760 mAh/g, which means that the maximum capacity can be delivered in 1 h during cycling.
[36] S. Laruelle, S. Grugeon, P. Poizot, M. Dolle, L. Dupont, J.-M. Tarascon, J. Electrochem. Soc. 149 (2002) A627.
[37] F. Gillot, S. Boyanov, L. Dupont, M.-L. Doublet, M. Morcrette, L. Monconduit, J.-M. Tarascon, Chem. Mater. 17 (2005) 6327.
[38] S. Boyanov, J. Bernardi, E. Bekaert, M. Menetrier, M.-L. Doublet, L. Monconduit, Chem. Mater. 21 (2009) 298.
[39] D. Guyomard, C. Sigala, A. Le Gal La Salle, Y. Piffard, J. Power Sources 68 (1997) 692.
[40] B. Das, M.V. Reddy, C. Krishnamoorthi, S. Tripathy, R. Mahendiran, G.V. Subba Rao, B.V.R. Chowdari, Electrochim. Acta 54 (2009) 3360.